ELSEVIER

Journal of Structural Geology 29 (2007) 59–72

JOURNAL OF STRUCTURAL GEOLOGY

www.elsevier.com/locate/jsg

Influence of early strike-slip deformation on subsequent perpendicular shortening: An experimental approach

Ruth Soto [a,*], Joseph Martinod [b], Francis Odonne [b]

[a] *Departamento de Física, Escuela Politécnica Superior, Universidad de Burgos, av. Cantabria, 09006 Burgos, Spain*
[b] *LMTG – Université P. Sabatier, 14 Avenue Edouard Belin, 31400 Toulouse, France*

Received 15 March 2006; received in revised form 9 August 2006; accepted 18 August 2006
Available online 4 October 2006

Abstract

We used sandbox analogue models to study the influence of previous pure strike-slip and transpressional structures on subsequent perpendicular compression. We performed also a brittle–viscous system in order to analyse the presence of a viscous basal level. Experimental results show that a previous pattern generated under pure strike-slip and transpressive regime causes the reactivation of structures with favourable orientation and the nucleation of oblique thrusts and non-rectilinear deformation fronts under compression perpendicular to the first fault system. The presence of a viscous basal level with the imposed strain rate, which does not favour the coupling between the viscous layer and cover, inhibits the reactivation of previous structures. Comparison with a sector of Northern Chile margin (24–25°S), located in the forearc trench-parallel region supports the experimental results.

Keywords: Strike-slip; Transpression; Analogue models; Reactivation; Andean forearc deformation

1. Introduction

Inherited structural features represent a key factor in controlling strain distribution and localisation of deformation (e.g. Holdsworth et al., 2001), as surfaces of pre-existing faults display lower cohesive strength and friction coefficient than intact rocks (Anderson, 1951). Since the last decades, the importance of reactivation processes to obtain deformation trends oblique to the expected fault orientation is well known (e.g. Ranalli and Yin, 1990; Tikoff and Teyssier, 1994; Casas-Sainz, 1993; De Paola et al., 2005). Numerous previous experimental studies have been performed in order to analyse reactivation of pre-existing structures or the influence of pre-existing faults on the new created fault pattern, and most of them have dealt with tectonic inversion (e.g. McClay, 1989; Brun and Nalpas, 1996; Keep and McClay, 1997; Dubois et al., 2002; Panien et al., 2005). In the last years, a wide range of different reactivation processes have been analysed in order to study different processes, such as transpressional reactivation of normal faults (Ustaszewski et al., 2005) or reverse faults (e.g. Viola et al., 2004), or reactivation of normal faults in extension (Bellahsen and Daniel, 2005).

When an area has experimented superimposed tectonic regimes, one of the hardest task is to discriminate how previous structures have contributed to the latest tectonic regime. In this work, we study the effect of pure strike-slip and transpressional faults in a final configuration with compression perpendicular to the previous fault system. Strike-slip to reverse reactivation can occur in nature under different scenarios: (1) when σ_1 experiences a direction change because of variations in plate convergence and/or slab retreat (e.g. Betic chain, SE Spain; Sanz de Galdeano and Buforn, 2005) and (2) if plate convergence does not vary, in the forearc of oblique convergence subduction margins due to changes in the strain partitioning into parallel strike-slip faulting and orthogonal

* Corresponding author. Tel.: +34 947 258978; fax: +34 947 259349.
E-mail addresses: rsoto@unizar.es, rlsoto@ubu.es (R. Soto), martinod@lmtg.obs-mip.fr (J. Martinod), odonne@lmtg.obs-mip.fr (F. Odonne).

0191-8141/$ - see front matter © 2006 Elsevier Ltd. All rights reserved.
doi:10.1016/j.jsg.2006.08.001

thrusting (e.g. Chilean forearc). In order to validate the experimental results we have chosen a sector of Northern Chile margin (24–25°S) located in the forearc trench-parallel region that has registered strike-slip movements during the Eocene–Oligocene and perpendicular compression during the Neogene (Soto et al., 2005).

2. Experimental method

The experimental apparatus consisted of a large table (1.1 m × 0.8 m) on top of which lies a thin metallic plate linked to a computer-driven stepper motor (Fig. 1). Models did not present side walls in order to avoid sideways friction and were wide enough to allow a relatively large amount of deformation without edge effects. The mobile basal plate covered only one half of the table and had a rectangular shape for pure strike-slip deformation or forming a convergence angle (α) of 5° or 10° for transpressive deformation regime (Fig. 1 and Table 1). The moving boundary of this plate induced an asymmetric velocity discontinuity at the base of the models (e.g. Malavieille, 1984; Allemand et al., 1989), which localised the deformation in the covering sandpack (e.g. Richard, 1991b; Barrier et al., 2002). Models experimented two deformation stages: (1) pure strike-slip or transpression regime depending on the angle of the velocity discontinuity with respect to the bulk shear direction (i.e. convergence angle) (α) and (2) compression perpendicular to the previous velocity discontinuity. Reference model PN-04 was performed with a viscous décollement layer only in the central part of the experiment and only compressional motion (perpendicular to the velocity discontinuity) in order to compare how a previous fault system influences the resulting fault pattern with and without viscous décollement level. Two different setups have been used in analogue modelling in order to analyse the influence of a previous fault or fault network: (1) creating discontinuities by introducing a piece of cardboard or a metallic wire in the sandcake (Viola et al., 2004; Bellahsen and Daniel, 2005) or (2) subjecting models to two consecutive and different stages of deformation (e.g. Dubois et al., 2002; Ustaszewski et al., 2005). In this work, we have chosen the second case (i.e. performing two consecutive stages of deformation) due to the helicoidal geometry of strike-slip faults (i.e. Riedel faults) (Naylor et al., 1986), very difficult to simulate using a piece of cardboard or a metallic wire.

Simple sandpack models made of dry eolian quartz Fontainebleau sand (small cohesion, density $\rho = 1.493\ \mathrm{g\,cm^{-3}}$; Krantz, 1991) were made to simulate the brittle behaviour of the upper crust. Its deformation is considered as effectively time independent (Hubbert, 1937). Only models PN-04 and PN-05 presented a 30 cm long, 8 cm wide and 0.5 cm thick and 40 cm long, 8 cm wide and 0.5 cm thick, respectively, basal silicone putty layer. We used this layer, as in previous studies, to simulate the behaviour of a viscous detachment level (e.g. Vendeville, 1987; Cobbold et al., 1989; Richard, 1991b; Weijermars et al., 1993). The silicone putty used is a nearly Newtonian fluid with a density of $0.97\ \mathrm{g\,cm^{-3}}$ and a viscosity of 1×10^4 Pa s at room temperature for the deformation velocity of $4\ \mathrm{cm\,h^{-1}}$ used during the experiment. Models were scaled in terms of gravitational forces, rheology, and strain rates (Hubbert, 1937; Ramberg, 1981; Casas et al., 2001). The model ratio for length is 10^{-5} (1 cm in the model represents 1 km in nature); for stress, 10^{-5} (models are 10^5 times weaker than nature); for time 10^{-9} (1 h represents 100 000 years). All models run at $4\ \mathrm{cm\,h^{-1}}$. One-layer sandpack and two-layer (silicone-sand) models experimented 20 mm and 25 mm of dextral strike-slip component displacement during the first stage of deformation, respectively, and 10 mm of shortening during the second stage of deformation. In the reference model PN-04, we applied only 1 cm of shortening in compressional motion perpendicular to the velocity discontinuity.

During experiments, in order to analyse the progressive evolution of structures we took photographs of the surface of models at regular intervals. At the end of the two deformational stages, serial cross-sections perpendicular to the basal velocity discontinuity showed the three-dimensional geometry

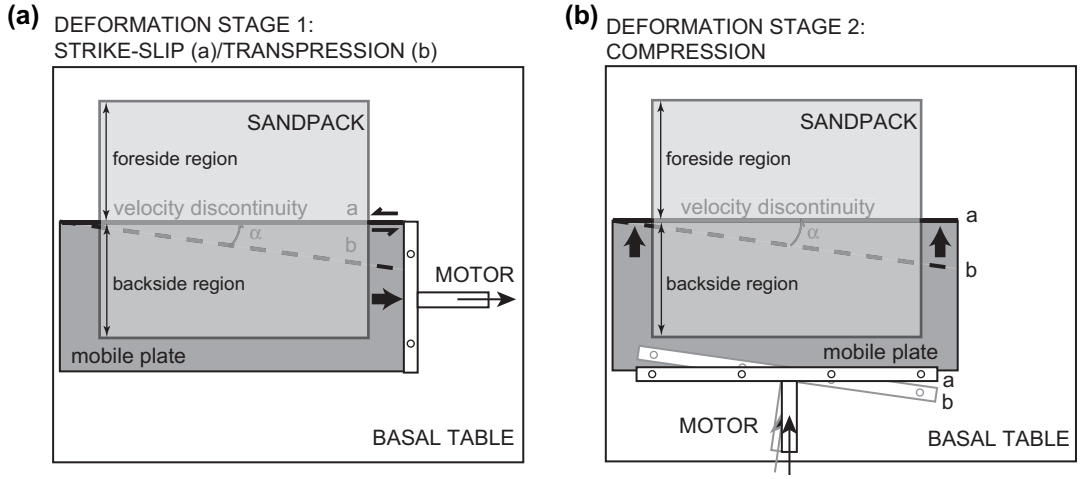

Fig. 1. Experimental apparatus. (a) Plan view of the apparatus during the first stage of deformation. Note the variation of the angle of convergence (α) from pure strike-slip faulting ($\alpha = 0°$) to moderate transpressive faulting ($\alpha = 5–10°$). (b) Plan view of the apparatus during the second stage of deformation, compression, which is perpendicular to the previous velocity discontinuity.

Table 1
Initial configuration of experiments

Model	Sandpack thickness (cm)	Silicone thickness (cm)	Displacement rate (cm h^{-1})	Deformation stage 1 (displacement)	Convergence angle, α (°)	Deformation stage 2 (displacement)
PN-01	3.5	–	4	Strike-slip (20 mm)	0	Compression (10 mm)
PN-02	3	–	4	Transpression (20 mm)	5	Compression (10 mm)
PN-03	3	–	4	Transpression (20 mm)	10	Compression (10 mm)
PN-04	2.5	0.5	4	–	0	Compression (10 mm)
PN-05	2.5	0.5	4	Strike-slip (25 mm)	0	Compression (10 mm)

of the internal structures. The total pre-kinematic thickness was 3.5 cm for PN-01 and 3 cm for the rest of models. In order to have a thorough understanding of the role of pre-existing pure strike-slip and transpression structures on the geometry and kinematics of posterior structures formed under compression, we prepared the sequence of models to study the effect of two principal variables (Table 1): (1) the variation of the angle of convergence (α) from the pure strike-slip system ($\alpha = 0°$) to moderate transpressive experiments ($\alpha = 5–10°$) during the first stage of deformation, and (2) the presence or absence of a viscous detachment level at the base of the model. Models are described using the following geodynamic framework: the backside is the region located on the mobile plate and foreside is located on the fixed plate (Fig. 1).

3. Compression perpendicular to pure strike-slip structures

In order to investigate the effects of basement fault reactivation on the deformation of a brittle sedimentary cover with/without a basal viscous décollement layer, we built sand and sand-silicone models. In the laboratory we applied two successive deformation stages: an initial phase of pure strike-slip motion and a subsequent phase of compression perpendicular to the velocity discontinuity (Fig. 1).

3.1. First stage: pure strike-slip deformation

Deformation during the first stage in pure strike-slip model without viscous detachment level (model PN-01; sand only) follows the evolution of similar sandbox model experiments (e.g. Naylor et al., 1986; Viola et al., 2004; Le Guerroué and Cobbold, 2006) (Fig. 2): (i) the deformed area is located above the basal velocity discontinuity (Fig. 2a), (ii) *en échelon* synthetic Riedel shears appear ranged between 27° and 28° with respect to the bulk shear direction during early stages of deformation (Fig. 2a). Riedel shears first develop in the external part of the model, probably due to edge effects, and with increasing displacement, also nucleate in the middle part, and (iii) with increasing offset, Y-type faults subparallel to the bulk shear direction develop. As a result, anastomosing shear zones develop isolating lenses (Fig. 2b). Riedel faults in cross-section are straight or convex-upward describing a flower shape and their three-dimensional geometry displays a helicoidal shape (see also Naylor et al., 1986); they have steep dips coinciding with the velocity discontinuity, where the strikes form around 30° to the basement discontinuity and with increasing the distance to the velocity discontinuity their dips diminish and their trends turn parallel to the basement discontinuity direction (Fig. 2).

Model underlain a silicone layer (model PN-05; sand-silicone) experiments a similar evolution with some differences with respect to one-layer-sandpack model (Fig. 3): (i) the range of *en échelon* synthetic Riedel faults needs higher amount of sinistral displacement to nucleate because higher bulk shearing of the overburden accommodates deformation during the early stages of deformation. This causes higher vertical axis rotation in the deformed area (see marker lines on the surface of the model in Fig. 3a) comparing with model without basal viscous décollement. Consequently, in pure strike-slip regimes and under basal frictional conditions, the deformed area shows smaller vertical axis rotations when compared with basal viscous detachment scenarios, and (ii) the size and spacing of single Riedel faults are smaller compared to model without viscous detachment level (Fig. 3a).

3.2. Second stage: compression deformation

The evolution of structures accreted from horizontal one-layer and two-layer silicone-sand cakes and pure convergence perpendicular to the velocity discontinuity without any previous fault pattern (as the reference model PN-04; Fig. 4) is well described in the literature (e.g. Tondji Biyo, 1995; Storti, 1997; Barrier et al., 2002). Without an underlain viscous layer (i.e. in the external parts of model PN-04), the first-order growth progressed by a homogeneous layer-parallel shortening in the region close to the velocity discontinuity, followed by the formation of two conjugate reverse faults that define a pop-up structure asymmetric forelandwards (i.e. towards the foreside) (Fig. 4). The dip angles of these faults in the foreside and backside are 25.5° and 34.5°, respectively (Fig. 4c). With basal viscous décollement (i.e. in the central part of model PN-04), deformation migrates forelandwards towards the end of the viscous layer where a symmetric pop-up structure develops (Fig. 4). In plan view, the main geometric feature is that deformation fronts show almost rectilinear traces, striking perpendicular to the direction of compression (i.e. parallel to the velocity discontinuity).

However, under basal frictional conditions, if pre-existing structures resulted from a previous pure strike-slip regime are present, the subsequent fault pattern varies considerably (Fig. 2d). Segments of the Riedel faults located on the mobile plate are reactivated as oblique thrusts. They progress laterally, first as oblique thrusts and then as thrusts. Simultaneously,

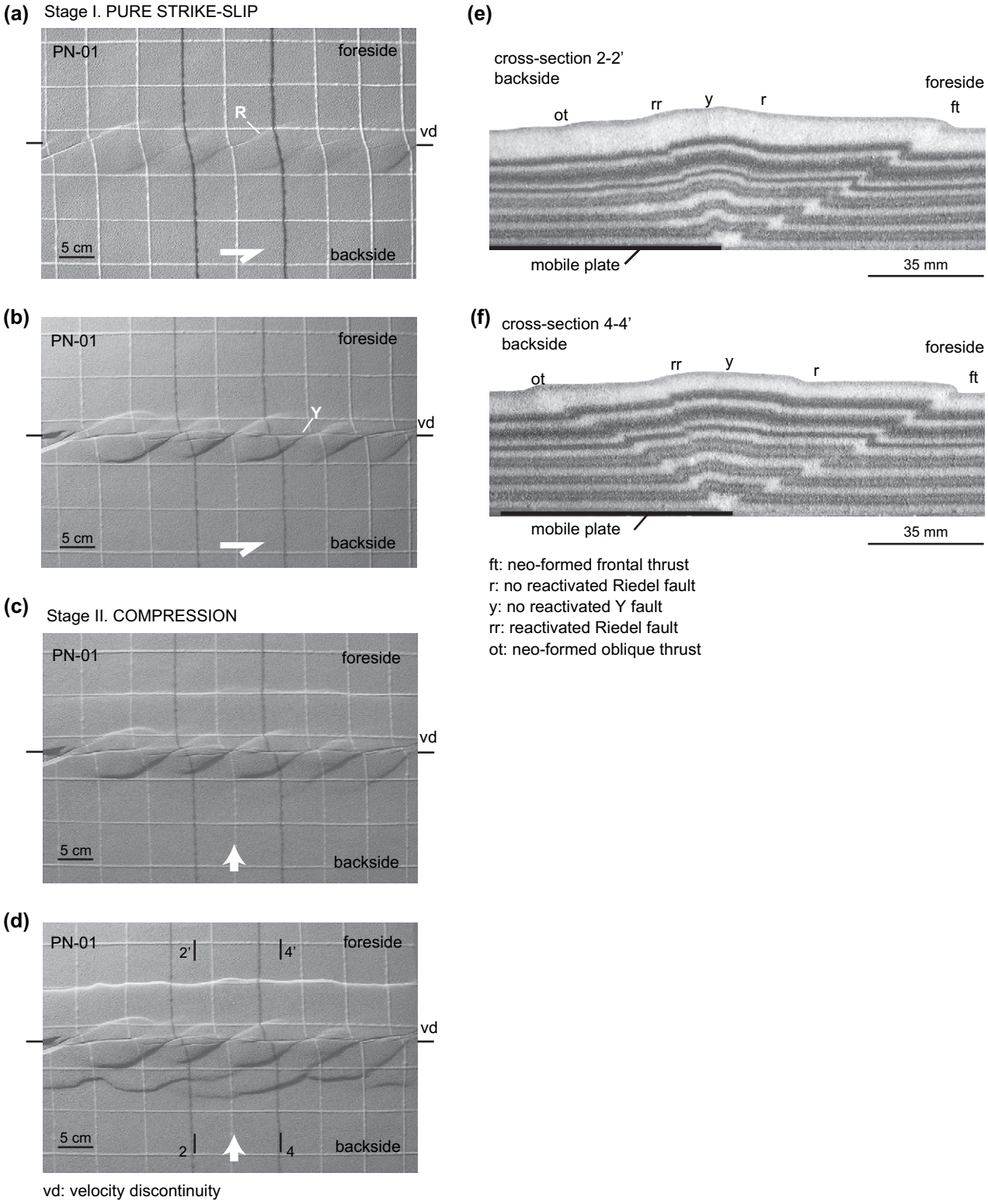

Fig. 2. Map view photographs of sequential evolutionary stages of experiment PN-01 after 10 mm (a) and 20 mm (b) of pure strike-slip displacement (Stage I) and 5 mm (c) and 10 mm (d) of shortening perpendicular to the velocity discontinuity (Stage II). White arrows are drawn over the mobile plate and show its sense and direction of motion. (e, f) Cross-sections of model PN-01 perpendicular to velocity discontinuity after the two stages of deformation.

at the foreside of the model, Riedel faults experiment minor reactivation and a frontal thrust parallel to the velocity discontinuity accommodates almost all the deformation (Fig. 2).

In order to analyze the 3D geometry of structures of model PN-01 (sand only), we measured the dip angle of the Riedel shears from cross-sections perpendicular to the velocity discontinuity after the two stages of deformation (i.e. pure-strike

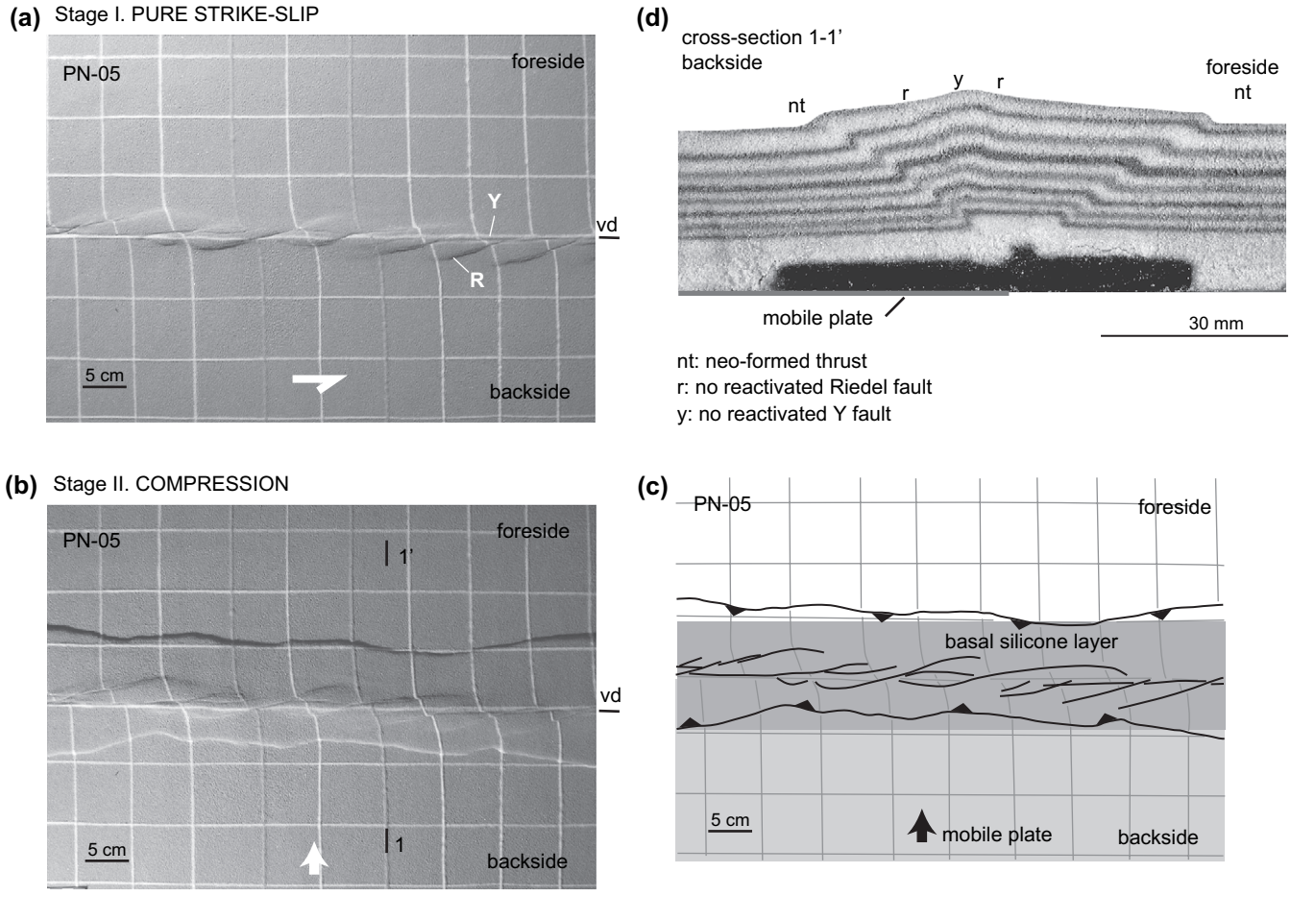

Fig. 3. Map view photographs of sequential evolutionary stages of experiment PN-05 (sand-silicone model) after 25 mm (a) of pure strike-slip displacement (Stage I) and 10 mm (b) of shortening perpendicular to the velocity discontinuity (Stage II). White arrows are drawn over the mobile plate and show its sense and direction of motion. (c) Line-drawing from (b) showing the initial position of the basal silicone layer. (d) Cross-section of model PN-05 perpendicular to velocity discontinuity after the two stages of deformation.

slip and compression). As they are oblique structures, the measured value of the dip angle is slightly lower than the real value (i.e. apparent dip angle). Fig. 5a shows that the dip angle of the Riedel faults diminishes with the distance from the velocity discontinuity, following an almost linear relationship. Segments of the Riedel faults located in the foreside sector of the model display higher dip angles because they experiment a horizontal-axis tilting related to the frontal fore-thrust advance (see cross-sections on Fig. 2). Fig. 5b shows that oblique thrusts nucleated from Riedel faults at the backside of model PN-01 present lower dip angles than Riedel faults but higher dip angles with respect to thrust dips. As for Riedel faults, the dip angle of these oblique faults also diminishes with the distance from the velocity discontinuity (Fig. 5b). Riedel faults generally display convex-upward shape from cross-sections (Fig. 6). However, the geometry of faults nucleated from Riedel faults during the compressional stage varies along-strike from convex-upward shape coinciding with oblique thrusts to concave-upward or straight shapes when they become thrust segments parallel to the velocity discontinuity (Fig. 6). To conclude, experimental results show that a previous fault pattern generated under pure strike-slip conditions strongly influences the geometry of new formed thrusts, generated in compressional scenarios and under frictional basal conditions; Riedel faults are reactivated and the new thrusts nucleated from their terminations are oblique ramps with high dip angles.

In the model underlain a silicone layer (PN-05), the situation during the second stage of compressional deformation is completely different from model under frictional basal conditions. No structure is reactivated and two new thrusts appear, parallel to the velocity discontinuity in the foreside and backside (Fig. 3). The thrust-system position, however, is influenced by the pre-existing faults. Its base nucleates close to Riedel faults (Fig. 3d) and not at the viscous layer boundary as in experiment PN-04 (reference model) (Fig. 4d). The backside thrust nucleates closer to the Riedel faults generated in the first stage of deformation than the frontal thrust in the foreside. Both deformational fronts are not rectilinear describing various small salients and recesses. The thrust in the backside displays a more sinuous geometry and three segments appear parallel to the Riedel faults trend. This configuration is different from model PN-04, also with a basal viscous layer in its central part, but without any previous strike-slip deformation, since in model PN-04 deformation propagates towards the end of the viscous layer in the foreside and the structures that form

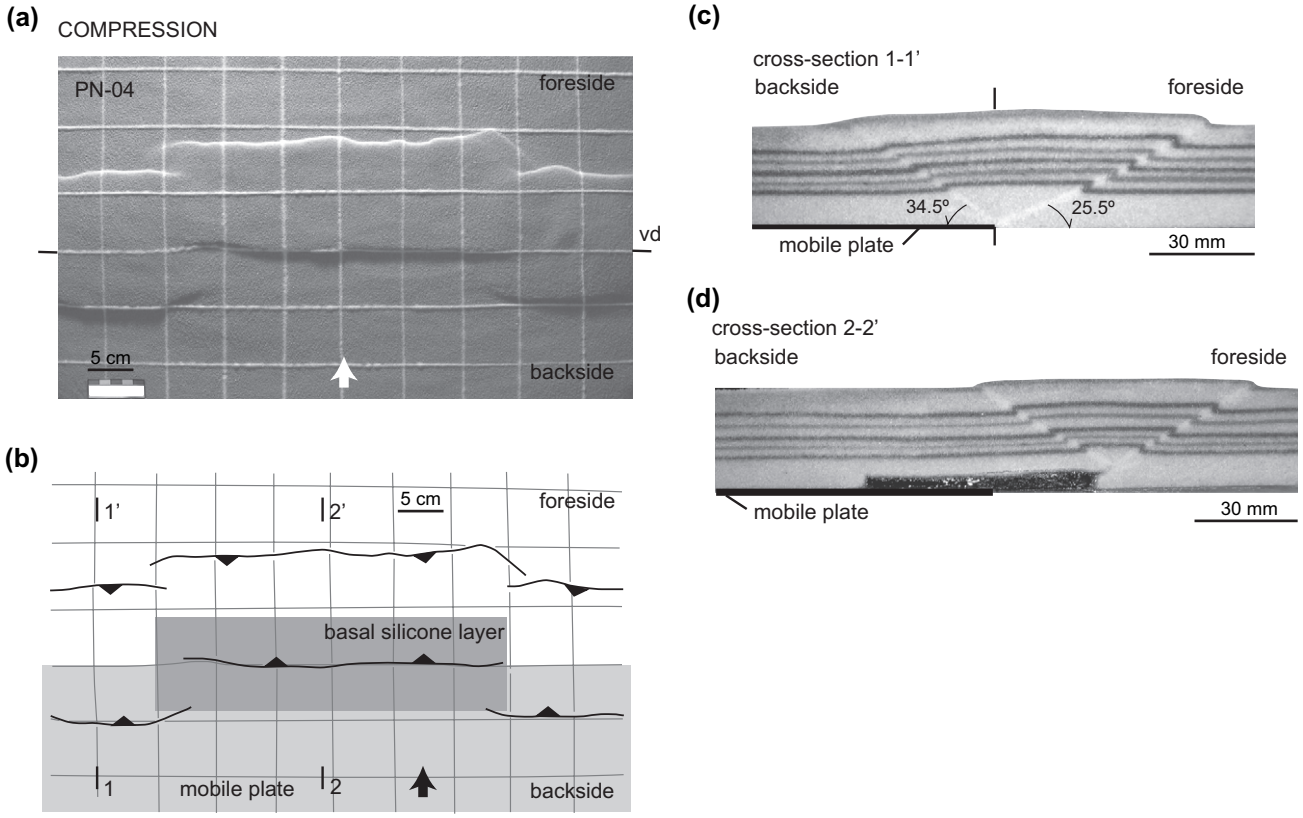

Fig. 4. (a) Map view photograph of experiment PN-04 (reference model) after 10 mm of shortening perpendicular to the velocity discontinuity. White arrow is drawn over the mobile plate and shows the sense and direction of motion of the mobile plate. (b) Line-drawing from (a) showing the initial position of the basal silicone layer. (c, d) Cross-sections of model PN-04 perpendicular to velocity discontinuity after compression under basal frictional and viscous conditions, respectively.

the pop-up are rectilinear. This indicates that despite any previous structure reactivated, the pre-existing fault network influenced the fault pattern formed during shortening.

4. Compression perpendicular to transpressional structures

In this case, only sandpack models were performed applying also two successive deformation stages: an initial phase of transpression varying the angle of convergence (α) between 5° and 10° and a posterior phase of compression perpendicular to the velocity discontinuity (Fig. 1).

4.1. First stage: transpressional deformation

We achieved transpression imposing the shear motion oblique with respect to the velocity discontinuity following the configuration performed by Viola et al. (2004). The angle of convergence is 5° and 10° for PN-02 and PN-03, respectively, values responding to wrench-dominated transpression versus thrust-dominated transpression models (Fossen et al., 1994; Tikoff and Teyssier, 1994; Casas et al., 2001). As can be seen from Figs. 7 and 8, both experiments follow a similar evolution. Before 0.8 cm and 1 cm of shortening for PN-02 and PN-03, respectively, models experiment only a bulk shearing and a fold appears, parallel to the velocity discontinuity trend. Then, an oblique-slip reverse thrust with sinistral component nucleates in the backside of models and a series of *en échelon* Riedel faults appear. In the central sector of models, Riedel faults nucleate at 26° and 29° with respect to the velocity discontinuity trend for PN-02 and PN-03, respectively. At the foreside of models, Riedel faults progress as thrusts with lateral component parallel to the basement discontinuity direction.

Increasing the angle of convergence from 5° (model PN-02) to 10° (model PN-03) diminishes wrenching conditions, resulting in a smaller number of Riedel faults. After 1.5 cm of shortening, while the deformation front in the backside is well defined in both models, it is characterised in the foreside by individual segments of reverse thrusts linked to the termination of Riedel faults. Only in model PN-03, after 1.8 cm of displacement, they merge along-strike to form a well-defined reverse fault with lateral component in the foreside. Deformational fronts at the foreside and backside of models are parallel to the velocity discontinuity but they are not rectilinear. They display a sinuous shape formed by small salients influenced by the Riedel faults location.

4.2. Second stage; compression deformation

Following the first stage of transpression, models PN-02 and PN-03 are deformed by compression. We choose compression perpendicular to the velocity discontinuity in order to have the simplest scenario (i.e. without wrenching conditions)

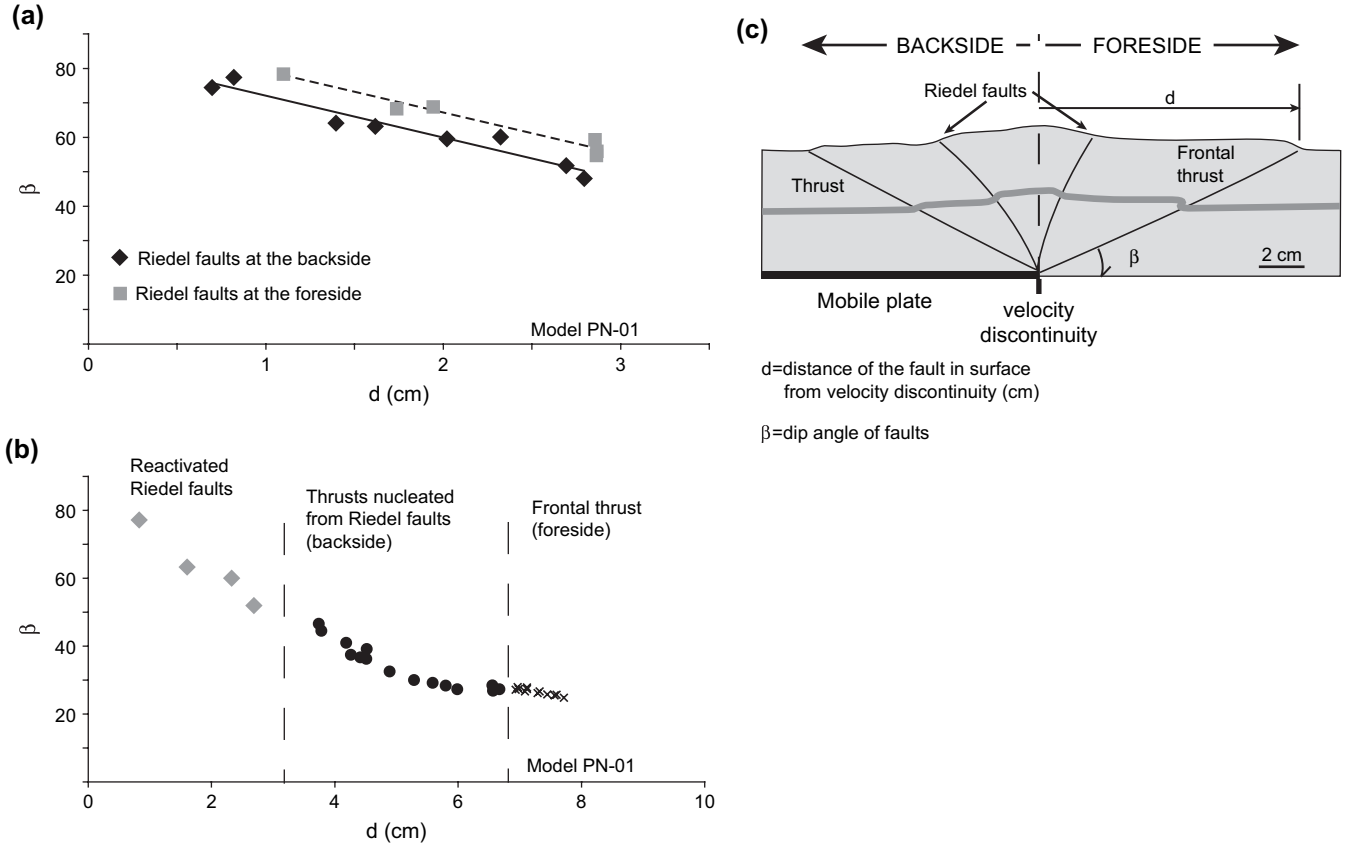

Fig. 5. (a) Plots of the dip angle (β) of Riedel faults in the foreside and backside of model PN-01 and the dip angle of Riedel faults; (b) dip angle of oblique thrusts nucleated from Riedel faults in the backside and frontal thrust in the foreside of model PN-01 versus the distance of these faults in surface from the velocity discontinuity. (c) Line-drawing of cross-section perpendicular to the velocity discontinuity of model PN-01 showing the measured parameters.

for studying reactivation processes. In the early stages of shortening, a new frontal thrust generated in the foreside of both models parallel to the preceding deformation front. In the backside sector, in contrast, no new structure formed and the previous transpressional deformation front reactivated (Figs. 7 and 8) resulting in an asymmetric fault pattern. In both models, the new frontal thrust is not rectilinear, adopting a sinuous geometry in plan view similar to that of the backside reactivated deformation front. Cross-sections on Figs. 7 and 8 show that the Riedel faults had a limited reverse component above the basement discontinuity in both models versus the sinistral strike-slip offset deduced from plan view.

5. Comparing pure strike-slip and transpressive models with posterior compression

Regarding the first stage of deformation, pure strike-slip and transpressive models display some differences already described by Casas et al. (2001). The main features that differentiate pure strike-slip from transpression scenarios are the following (Figs. 2, 7 and 8): (1) the number of Riedel faults and the deformation they accommodate diminish as the convergence angle (α) of the mobile plate increases; (2) only in transpressional conditions, the deformation zone shows a pop-up geometry bounded by two conjugate reverse thrusts parallel to the velocity discontinuity and slightly asymmetric towards the mobile plate. These differences determine strongly the fault pattern generated during the subsequent compressional stage. Thus, only in the experiment with previous pure strike-slip structures, Riedel faults are reactivated and oblique thrusts form on the mobile plate during compression. As cross-sections show, the presence of pure strike-slip structures results in a more symmetric deformation zone as compared with transpressive models (Figs. 2, 7 and 8). A common feature in all models, either with previous pure strike-slip or transpressive structures, is the reactivation of structures located on the mobile plate (i.e. backside) in contrast with minor or no reactivation on the fixed plate (i.e. foreside). This differential behaviour, reactivation only in the backside, implies the nucleation at the foreside of all models of a frontal thrust that accommodates the deformation (Figs. 2, 7 and 8).

6. Discussion

6.1. Reverse reactivation of pre-existing pure strike-slip or transpressional structures

From previous analytical and experimental works, it is known that reactivation depends on the dip and strike of the pre-existing faults (e.g. Ranalli and Yin, 1990; Yin and Ranalli, 1992; Dubois et al., 2002; Viola et al., 2004) and also on the pre-existing fault network (Bellahsen and Daniel,

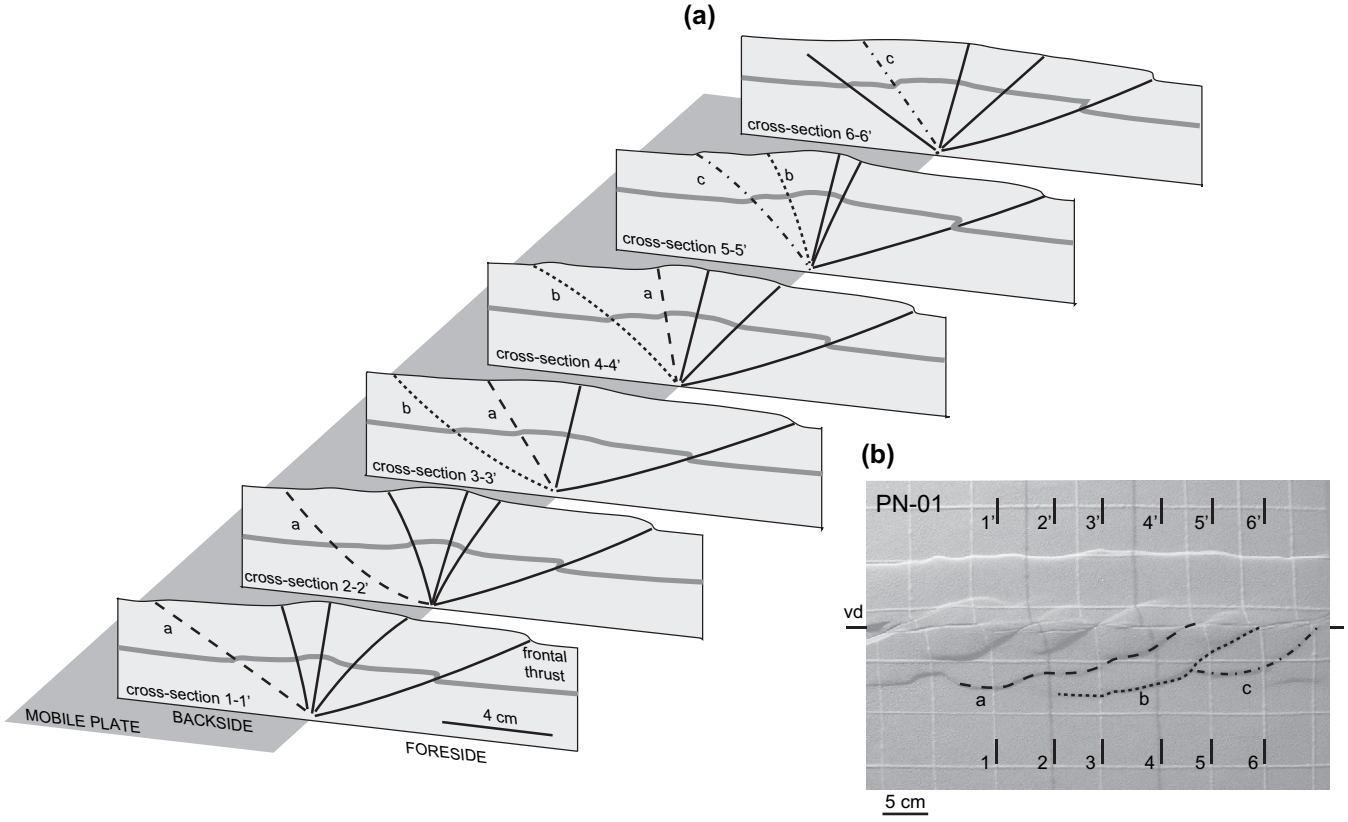

Fig. 6. (a) Serial cross-sections at the end of model PN-01 showing its internal architecture and the along-strike variability of the geometry of Riedel and thrusts in the backside of the model. (b) Map view photograph of experiment PN-01 showing cross-section location and faults.

2005). Our results confirm that the geometry of new formed thrusts during compression is strongly influenced by the geometry of the pre-existing structures and also by the existence of a basal viscous layer. Thus, favourably oriented strike-slip structures reactivate in the form of curved and/or oblique thrusts and non-rectilinear deformation fronts under perpendicular compression.

In our models, two kinds of pre-existing discontinuities influence their final configuration: the discontinuity formed by the edge of the mobile plate and the fault planes formed during the first deformation stage. The first one is basal, whereas the other discontinuities are located in the cover. The basal discontinuity controls all the shear strain localisation, therefore the location of structures during the first tectonic regime (e.g. Richard, 1991a), whereas during the second phase of shortening, both kinds of discontinuities influence; the basal one localises the deformation at the basement level, and the fault planes control its upward propagation.

In the experiments performed in this work, only faults located on the mobile plate (i.e. backside) reactivated in absence of viscous detachment layer. The reason lies in the orientation of the principal stress axes following the Coulomb failure criterion: toward the foreland, verging plane dips are shallower than does backwards (Hafner, 1951; see also Fig. 4c). This explains why only backside faults are reactivated during compression in our models. They present a more favourable orientation (i.e. higher dip angle closer to the dip of the potential steeper backthrusts). However, strike-slip structures formed previously in the foreside are too steep to be reactivated with the nucleation of potential less steep forethrusts.

6.2. Influence of an underlain viscous layer

When a viscous detachment level is present, no structure is reactivated in our experimental configuration despite the fact that the thrust-system location is influenced by the position of pre-existing faults. The capacity of viscous layers to propagate and accommodate shortening by ductile, i.e. not localised, deformation must probably inhibit the reactivation of previous structures. Ustaszewski et al. (2005) have also revealed minor reactivation processes in low displacement rate brittle–viscous experiments.

Our work does not imply that reactivation does not occur in presence of a viscous detachment layer in other situations. In fact, previous authors have studied this phenomenon and fault reactivation in strike-slip mode may occur at depth (Richard, 1991; Richard 1991b) or reactivation of normal faults during coaxial or oblique deformation takes place (Dubois et al., 2002) in presence of a viscous layer. Recently, Ustaszewski et al. (2005) have analysed this phenomenon for transtensional systems reactivated by transpressional wrench faulting. They suggest that under basal viscous conditions, the reactivation of pre-existing structures is strongly dependent on the coupling between viscous horizons and cover. This coupling depends on the strain rate (e.g. Ustaszewski et al., 2005) and

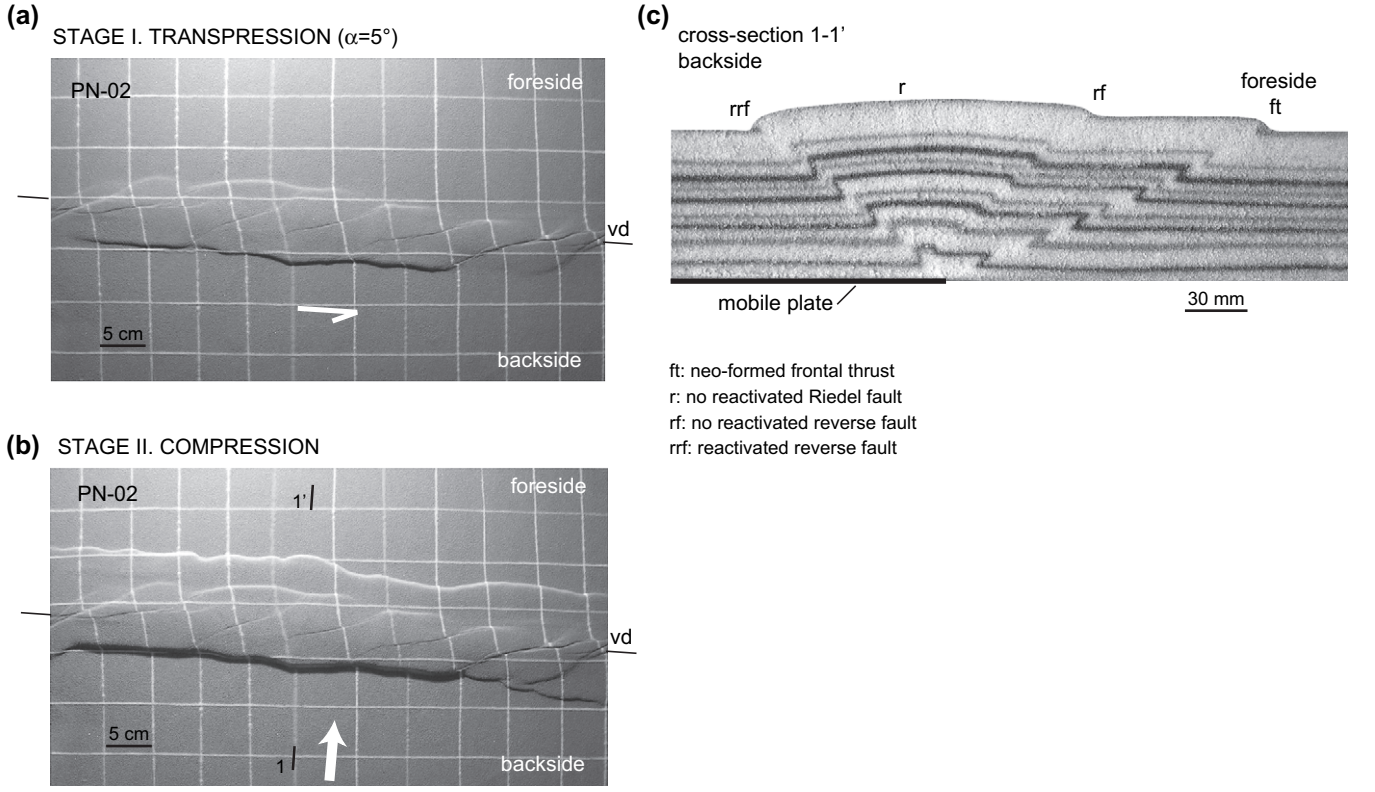

Fig. 7. Map view photographs of sequential evolutionary stages of experiment PN-02 after 20 mm (a) of transpression displacement (convergence angle, $\alpha = 5°$) (Stage I) and 10 mm (b) of shortening perpendicular to the velocity discontinuity (Stage II). White arrows are drawn over the mobile plate and show its sense and direction of motion. (c) Cross-section of model PN-02 perpendicular to velocity discontinuity after the two stages of deformation.

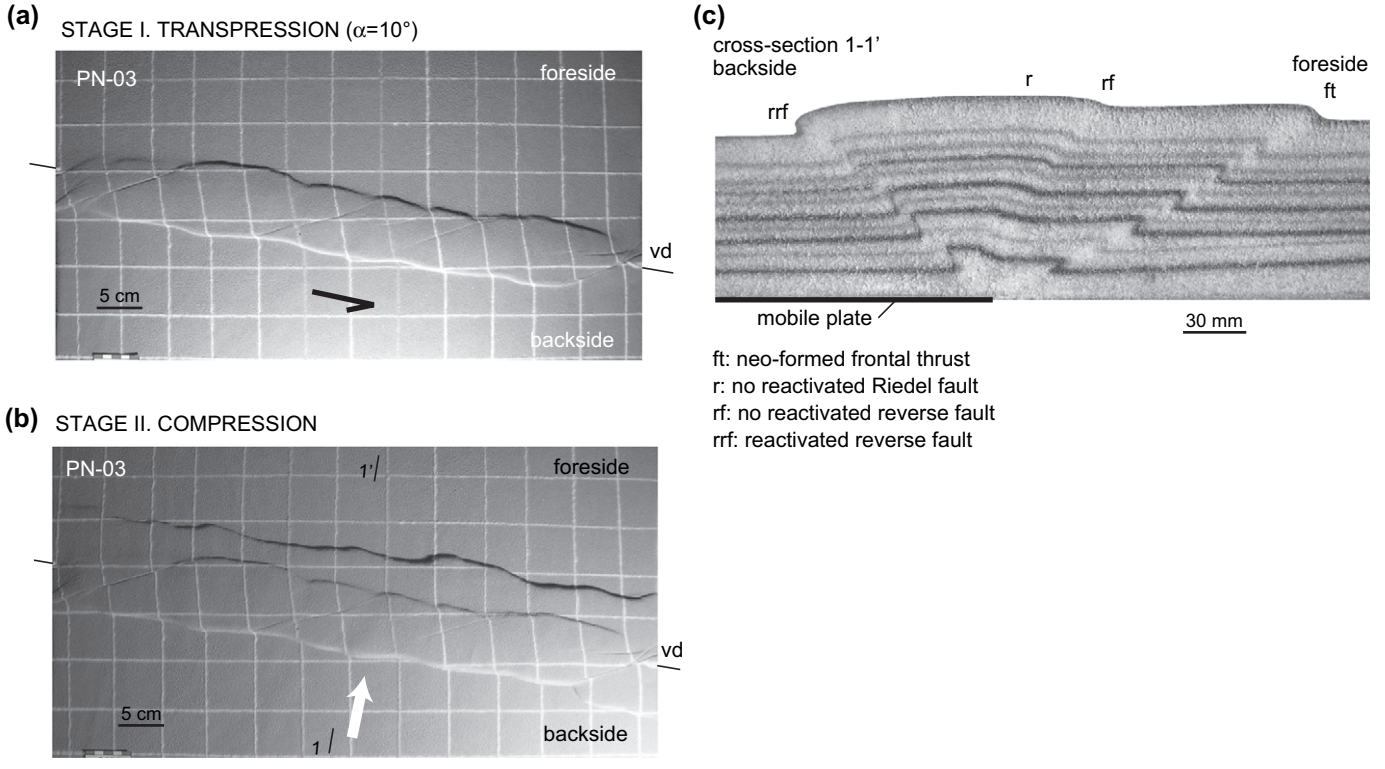

Fig. 8. Map view photographs of sequential evolutionary stages of experiment PN-03 after 20 mm (a) of transpression displacement (convergence angle, $\alpha = 10°$) (Stage I) and 10 mm (b) of shortening perpendicular to the velocity discontinuity (Stage II). White arrows are drawn over the mobile plate and show its sense and direction of motion. (c) Cross-section of model PN-03 perpendicular to velocity discontinuity after the two stages of deformation.

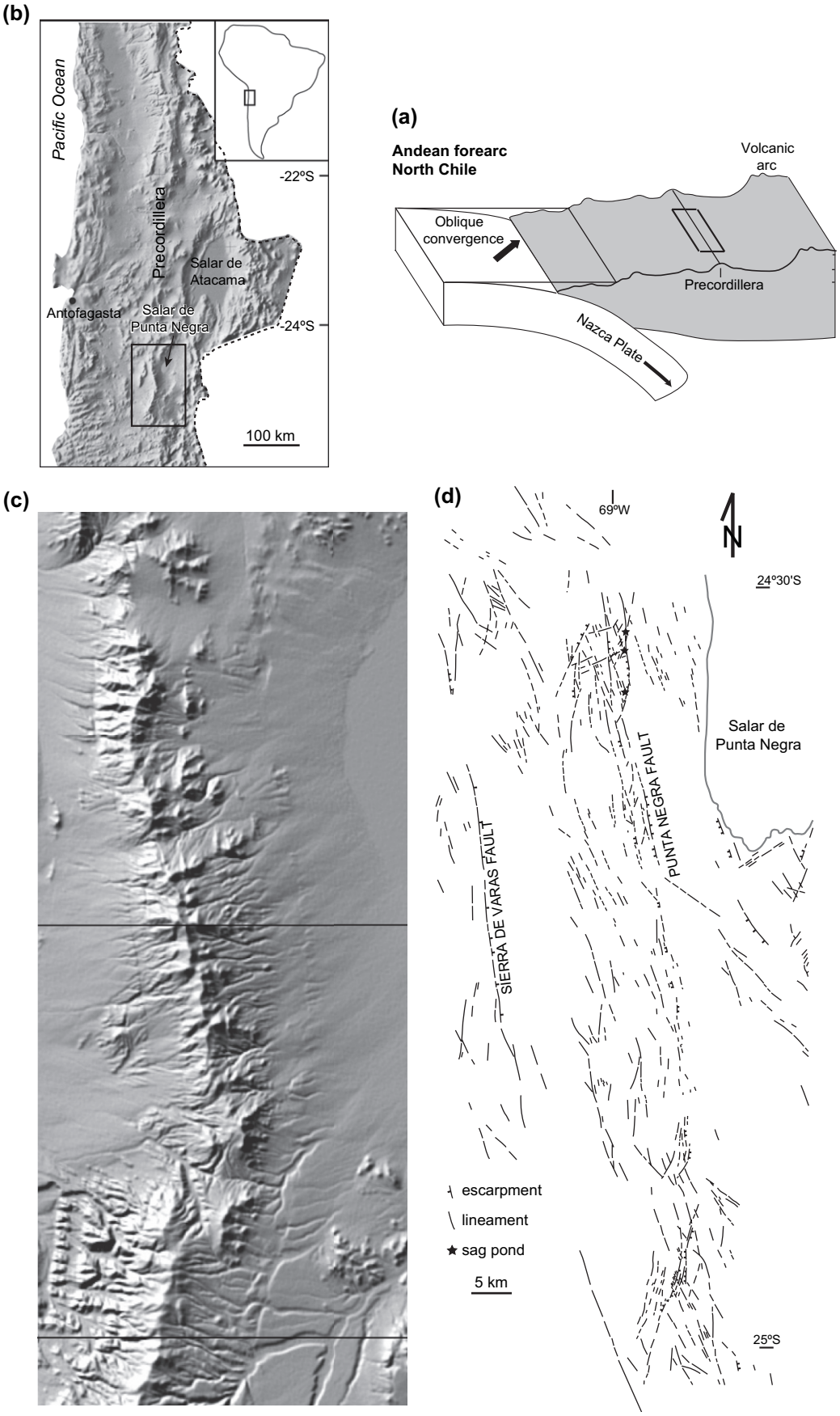

Fig. 9. (a) Schematic showing the oblique convergence of the Chilean margin and location of the Precordillera. (b) Location of the study area in the North Chilean forearc. (c, d) SRTM 90m Digital Elevation Model and photogeological interpretation from 1:50 000 aerial photographs and ASTER satellite images of lineaments affecting post-Miocene deposits from Soto et al. (2005).

the relationship between the thickness of the viscous material and the frictional overburden (e.g. Chapple, 1978; Davy and Cobbold, 1991). Thus, higher displacement rates and/or thinner viscous layers facilitate this coupling and reactivation of previous structures.

6.3. Comparison with previous works

Reactivation is a common process in nature, but it is many times a neglected factor in analogue and numerical studies. Many authors have performed laboratory experiments isolating tectonic regimes as pure strike-slip deformation (e.g. Naylor et al., 1986; Richard and Cobbold, 1989; Schöpfer and Steyrer, 2001), transpressive systems (e.g. Fossen and Tikoff, 1998; Schreurs and Colletta, 1998; Casas et al., 2001) or pure compressional deformation (e.g. Storti, 1997; Nalpas et al., 1999; Barrier et al., 2002). During the last decades, numerous analogue experiments have studied the effect of two successive tectonic regimes in order to analyse the influence of a previous fault set in the geometry and kinematics of the secondly formed structures and/or reactivation procceses. Most of them have dealt with tectonic inversion resulting from coaxial (e.g. McClay, 1989; Eisenstadt and Withjack, 1995; Faccenna et al., 1995) or oblique deformation (e.g. Brun and Nalpas, 1996; Keep and McClay, 1997; Dubois et al., 2002; Ustaszewski et al., 2005). Also fault reactivation of reverse faults in posterior strike-slip regimes has been simulated (Richard 1991b; Viola et al., 2004). Bellahsen and Daniel (2005) have analysed that reactivation depends not only on dip and strike of the pre-existing faults but also on the spatial organization on the structural heterogeneities. In this work, we study the effect of pure strike-slip and transpressional faults in a final configuration with compression perpendicular to the previous fault system trend.

6.4. Experimental limitations

The experiments performed include some oversimplifications of the pretectonic fabrics and syntectonic behaviour of natural scenarios. (1) Rheological and lithological changes due to palaeogeographic variations commonly occur in nature, despite the fact that our models were homogeneous sandpacks. (2) Interlayered detachment layers plays an important role in the deformational style (e.g. Davis and Engelder, 1985; Corrado et al., 1998; Ravaglia et al., 2004), whereas we imposed a single basal detachment in our models. (3) Syntectonic sedimentation and erosion take place in nature and influence the development of structures (e.g. Storti and McClay, 1995; Barrier et al., 2002; Casas et al., 2001; Gestain et al., 2004), but our models did not include the role of surface processes. (4) Our experiments did not take into account the circulation of synorogenic fluids within the growing structures, which is a first-order factor controlling the frictional behaviour of faults (Vannucchi, 1999).

However, although these experimental limitations mean that our models are not perfectly scaled analogues for natural situations as most analogue models, their results are still applicable to the first-order geodynamics of natural scenarios as observed in previous works (e.g. Naylor et al., 1986; Schreurs and Colletta, 1998; Casas et al., 2001; Viola et al., 2004).

7. Application to natural example: The Precordillera of Northern Chile (24–25°S), Central Andes

7.1. Geological setting

Orogens accreted in obliquely converging margins may cause the strain partitioning of deformation into strike-slip faulting and orthogonal thrusting (e.g. McCaffrey, 1992; Tikoff and Teyssier, 1994; Allerton, 1998; Lallemand et al., 1999), although this process is still poorly understood (e.g. Chemenda et al., 2000). Along the western Chilean margin, forearc deformation varies with time and along-strike (Hoffmann-Rothe et al., 2004). Factors controlling the strain partitioning along the Chilean plate boundary are space and time dependent and probably linked to the variability of many influential factors such as the geometry of the subduction slab, subduction erosion at trench, subcrustal accretion or forces coming from inner zones. This phenomenon has carried the occurrence in the same area, as the Precordillera of North Chile, of different deformation events with the possible implication of reactivation processes along preexisting fault zones.

The Precordillera in the Northern Chile forearc represents a N–S thick-skinned basement range bounded by a system of reverse faults and blind thrusts with alternating vergence along-strike (Mpodozis and Ramos, 1989; Fig. 9a, b). It results from the inversion since the end of Early Cretaceous of a previous Mesozoic back-arc basin (Mpodozis and Ramos, 1989; Amilibia et al., 2000). A main episode of transpression is described during the Eocene–Oligocene linked to oblique convergence (e.g. Maksaev and Zentilli, 1988; Mpodozis et al., 1993). The Neogene tectonic deformation of the Precordillera in Northern Chile, between 20 and 28°S, is essentially characterised by the reactivation of major structures that formed during previous tectonic episodes, in particular during the Eocene (Reutter et al., 1993; Tomlinson et al., 1994; Kuhn, 2002; Audin et al., 2003). It varies significantly with latitude and remains small everywhere.

At the Salar de Punta Negra latitude (24–25°S; Fig. 9b), aerial photographs, satellite images and fieldwork data indicate the existence of surfaces formed after the deposition of a Lower Miocene ignimbrite (Río Frío ignimbrite, K-Ar dates range from 23 to 17 Ma; Naranjo and Cornejo, 1992) that are affected by numerous lineaments linked to fault scarps. The plan-view fault pattern geometry in the studied area displays an approximately N–S trend (173°N). Overall, the deformation zone is arranged parallel to the Precordillera range that can be considered a zone of mechanical weakness and preexisting faults within the forearc of Northern Chile due to its variable and episodic deformation history (extensional stage, tectonic inversion, strike-slip deformation). Faults are slightly curved in plan view and describe an intermediate lens. The rest of lineaments show a complex arrangement *en échelon* mostly

located on the eastern flank of the Precordillera, resulting in an asymmetric deformation zone (Fig. 9d). Two families of faults can be distinguished concerning their surface strike with respect to the principal fault trends in the eastern flank of the Precordillera: fault segments ranging between 12° and 15° that correspond to the majority and fault segments ranging between 30° and 45°. This plan-view geometry is analogous to the pattern of strike-slip faults in sinistral transpression scenarios (Mpodozis et al., 1993), in which secondary lineaments could correspond to R and P faults, respectively. Geomorphological evidences of tectonic activity show that the latest deformation episode in the study area rules out strike-slip motions (Soto et al., 2005), despite the fact that the plan-view geometry of these lineaments suggests a sinistral transpression scenario (Mpodozis et al., 1993) (Fig. 9). Geomorphological markers suggest Neogene E–W compressional tectonics (Soto et al., 2005) as other authors have proposed for equivalent areas north and southwards (e.g. Jordan et al., 2002; Audin et al., 2003).

7.2. Comparison with the experimental results

Although the comparison of experimental results with natural examples is not straightforward, partly because of the limitations of experimental analogues and partly because of the numerous factors involved in natural examples, some well-defined features corroborate the applicability of the analogue models presented to the north Chilean Precordillera example. The geometry and kinematic evolution of analogue models show some similarities with the main features characterizing the style of deformation of the Precordillera at the Salar de Punta Negra latitude (24–25°S). (1) Both in the Precordillera and experimental models, the deformation zone appears parallel to pre-existing faults. (2) The accommodation of shortening by ductile and not localised deformation due to the presence of a viscous layer in the stratigraphic series (i.e. salt, shales or clay levels), as the experiments show, did not occur in the natural example, where a regional viscous detachment level is absent in the upper crust (e.g. Mpodozis et al., 1993). (3) Overall, the deformation zone is not symmetric. In the studied area, a higher number of faults appear in the eastern flank of the Precordillera with respect to the western flank (Fig. 9). If we compare the nature example and the physical models, the fault pattern of model PN-01 (i.e. pure strike-slip deformation followed by compression, sand only) matches with the deformation style showed in this sector of the Precordillera; both show an asymmetric pattern with an array of oblique reverse faults only on one side (i.e. on the mobile plate in the model and on the eastern flank of the Precordillera) (Figs. 2 and 9).

One limitation related with the Chilean forearc deformation is to solve what is the origin of the Neogene tectonic activity in the Precordillera. Two opposite forces proceeding from both sides of the forearc could have influenced its tectonic evolution during Neogene times: (a) the subduction of the Nazca plate beneath the South America continent (e.g. Pardo-Casas and Molnar, 1987; Hartley et al., 2000) and (b) the uplift of the Altiplano-Puna (located to the east of the Precordillera) and crustal thickening since Middle Oligocene (Victor et al., 2004; Farías et al., 2005; Tassara, 2005). Experiment PN-01 shows that a higher number of structures forms on the mobile plate. Thus, taking into account the experimental results, we can support that the main contributor to deformation in the studied sector of the Precordillera during the Neogene comes from the east, i.e. as a result of the uplift of the Altiplano-Puna. Therefore, the Precordillera in the study area could accommodate deformation during the Neogene, as Victor et al. (2004) and Farías et al. (2005) have documented northwards, by a west-vergent reverse fault system. In the study area, the presence of the Salar de Punta Negra basin to the east could reflect that the Precordillera acts as a doubly vergent range at this latitude more than like a large monocline as model PN-01 shows (Fig. 2).

To conclude, our models validate the assumption that the Neogene tectonic activity in the Salar de Punta area may result from moderate shortening perpendicular to the trench that reactivates and is influenced by previous strike-slip structures.

8. Conclusions

Experimental results show the influence of the previous pattern generated under pure strike-slip and transpressive conditions on the geometry of new formed thrusts generated under compression perpendicular to the first fault system. Structures are reactivated only at the backside sector of the models in absence of a viscous detachment level. In pure strike-slip conditions even the Riedel faults are reactivated and new thrusts nucleate from these Riedel faults by oblique ramps with high dip angles.

A comparison with a sector of Northern Chile margin (24–25°S), located in the forearc trench-parallel region supports the experimental results. This sector registered strike-slip movements related to the strain partitioning due to the oblique convergence of the Nazca plate during the Eocene–Oligocene that has influenced the fault pattern resulting from moderate margin-normal shortening during the Neogene. The asymmetry of the fault pattern on both sides of the Precordillera suggests that surface deformation in that part of the Precordillera could accommodate the Neogene Altiplano-Puna plateau uplift.

Acknowledgements

Models were performed in the Analogue Modelling Laboratory of the LMTG – Paul Sabatier University (Toulouse, France). This work was supported by a *Post-Doctoral* grant and a research position for young scientists (‘‘Juan de la Cierva’’ program) of the Spanish Ministry of Education and Science to the first author. We are grateful to Bruno Vendeville and Atilla Aydin for helpful reviews that improved the manuscript.

References

Allemand, P., Brun, J.P., Davy, P., van den Driessche, J., 1989. Symetrie et asymetrie des rifts et mecanismes d’amincissement de la lithosphere

(Symmetry and asymmetry of rifts and mechanism of lithospheric thinning). Bulletin de la Societe Geologique de France 5, 445–451.

Allerton, S., 1998. Geometry and kinematics of vertical-axis rotations in fold and thrust belts. Tectonophysics 299, 15–30.

Amilibia, A., Sabat, F., Chong, G., Muñoz, J.A., Roca, E., Gelabert, B., 2000. Criterios de inversión tectónica: ejemplos de la Cordillera de Domeyko (II Región de Antofagasta). Actas IX Congreso Geológico Chileno 2, 548–552.

Anderson, E.M., 1951. The Dynamics of Faulting and Dyke Formation with Applications to Britain. Oliver and Boyd, Edinburgh.

Audin, L., Hérail, G., Riquelme, R., Darrozes, J., Martinod, J., Font, E., 2003. Geomorphic markers of faulting and neotectonic activity along the Western Andean margin, Northern Chile. Journal of Quaternary Science 18, 681–694.

Barrier, L., Nalpas, T., Gapais, D., Proust, J.N., Casas, A., Bourquin, S., 2002. Influence of syntectonic sedimentation on thrust geometry; field examples from the Iberian Chain (Spain) and analogue modelling. Sedimentary Geology 146, 91–104.

Bellahsen, N., Daniel, J.M., 2005. Fault reactivation control on normal fault growth: an experimental study. Journal of Structural Geology 27, 769–780.

Brun, J.P., Nalpas, T., 1996. Graben inversion in nature and experiments. Tectonics 15, 677–687.

Casas-Sainz, A.M., 1993. Oblique tectonic inversion and basement thrusting in the Cameros Massif (Northern Spain). Geodinamica Acta 6 (3), 202–216.

Casas, A.M., Gapais, D., Nalpas, T., Besnard, K., Román-Berdiel, T., 2001. Analogue models of transpressive systems. Journal of Structural Geology 23, 733–743.

Chapple, W.M., 1978. Mechanics of a thin-skinned fold and thrust belt. Geological Society of America Bulletin 89, 1189–1198.

Chemenda, A., Lallemand, S., Bokun, A., 2000. Strain partitioning and interplate friction in oblique subduction zones: constraints provided by experimental modeling. Journal of Geophysical Research 105 (B3), 5567–5581.

Cobbold, P.R., Rossello, E., Vendeville, B., 1989. Some experiments on interacting sedimentation and deformation above salt horizons. Bulletin de la Societe Geologique de France V, 453–460.

Corrado, S., Di Bucci, D., Naso, G., Faccenna, C., 1998. Influence of palaeogeography on thrust system geometries: an analogue modelling approach for the Abruzzi-Molise (Italy) case history. Tectonophysics 296, 437–453.

Davis, D.M., Engelder, T., 1985. The role of salt in fold- and thrust belts. Tectonophysics 119, 67–88.

Davy, P., Cobbold, P.R., 1991. Experiments on shortening of a 4-layer model of the continental lithosphere. Tectonophysics 188, 1–25.

De Paola, N., Holdsworth, R.E., McCaffrey, K.J.W., Barchi, M.R., 2005. Partitioned transtension: an alternative to basin inversion models. Journal of Structural Geology 27, 607–625.

Dubois, A., Odonne, F., Massonnat, G., Lebourg, T., Fabre, R., 2002. Analogue modelling of fault reactivation: tectonic inversion and oblique remobilisation of grabens. Journal of Structural Geology 24, 1741–1752.

Eisenstadt, G., Withjack, M.O., 1995. Estimating inversion; results from clay models. In: Buchanan, J.G., Buchanan, P.G. (Eds.), Basin Inversion. Geological Society of London, Special Publications 88, Geological Society, London, pp. 119–136.

Faccenna, C., Nalpas, T., Brun, J.P., Davy, P., Bosi, V., 1995. The influence of pre-existing thrust faults on normal fault geometry in nature and in experiments. Journal of Structural Geology 17, 1139–1149.

Farías, M., Charrier, R., Comte, D., Martinod, J., Hérail, G., 2005. Late Cenozoic deformation and uplift of the western flank of the Altiplano: evidence from the depositional, tectonic, and geomorphologic evolution and shallow seismic activity (Northern Chile at 19° 30' S). Tectonics 24, doi:10.1029/2004TC001667. TC4001.

Fossen, H., Tikoff, B., 1998. Extended models of transpression and transtension, and application to tectonic settings. In: Holdsworth, R.E., Strachan, R.A., Dewey, J.F. (Eds.), Continental Transpressional and Transtensional Tectonics. Geological Society of London, Special Publications 135, Geological Society, London, pp. 15–33.

Fossen, H., Tikoff, B., Teyssier, C., 1994. Strain modeling of transpression and transtensional deformation. Norsk Geologisk Tidsskrift 74, 134–145.

Gestain, V., Nalpas, T., Rouby, D., Barrier, L., 2004. Rôle des niveaux incompétents syncinématiques sur l'évolution des zones chevauchantes-modélisations analogiques. Bulletin de la Societe Geologique de France 175, 351–359.

Hafner, W., 1951. Stress distribution and faulting. Geological Society of American Bulletin 62, 373–398.

Hartley, A., May, G., Chong, G., Turner, P., Kape, S.J., Jolley, E., 2000. Development of a continental forearc: a Cenozoic example from the Central Andes, northern Chile. Geology 28 (4), 331–334.

Hoffmann-Rothe, A., Kukowski, N., Oncken, O., 2004. Phase dependent strain partitioning in obliquely convergent settings. Bolletino di Geofisica (GeoMod Extended Abstracts) 45, 93–97.

Holdsworth, R.E., Hand, M., Miller, J.A., Buick, I.S., 2001. Continental reactivation and reworking; an introduction. In: Miller, J.A., Holdsworth, R.E., Buick, I.S., Hand, M. (Eds.), Continental Reactivation and Reworking. Geological Society of London, Special Publications 184, Geological Society, London, pp. 1–12.

Hubbert, M.K., 1937. Theory of scale models as applied to the study of geologic structures. Geological Society of American Bulletin 48, 1459–1520.

Jordan, T., Muñoz, N., Hein, M., Lowenstein, T., Godfrey, L., Yu, J., 2002. Active faulting and folding without topographic expression in an evaporitic basin, Chile. Geological Society of American Bulletin 114, 1406–1421.

Keep, M., McClay, K.R., 1997. Analogue modelling of multiphase rift systems. Tectonophysics 273, 239–270.

Krantz, R.W., 1991. Measurements of friction coefficients and cohesion for faulting and fault reactivation in laboratory models using sand and mixtures. Tectonophysics 188, 203–207.

Kuhn, D., 2002. Fold and thrust belt structures and strike-slip faulting at the SE margin of the Salar de Atacama basin, Chilean Andes. Tectonics 21 (4), doi:10.1029/2001TC901042.

Lallemand, S., Liu, C.S., Dominguez, S., Schnuerle, P., Malavieille, J., 1999. Trench-parallel stretching and folding of forearc basins and lateral migration of the accretionary wedge in the southern Ryukyus; a case of strain partition caused by oblique convergence. Tectonics 18, 231–247.

Le Guerroué, E., Cobbold, P.R., 2006. Influence of erosion and sedimentation on strike-slip fault systems: insights from analogue models. Journal of Structural Geology 28, 421–430.

Maksaev, V., Zentilli, M., 1988. Marco metalogénico regional de los megadepósitos de tipo pórfido cuprífero del norte grande de Chile. Actas V Congreso Geológico Chileno 1, B181–B212.

Malavieille, J., 1984. Modelisation experimentale des chevauments imbriques: application aux chaines de montagnes. Bulletin de la Societe Geologique de France 26, 129–138.

McCaffrey, R., 1992. Oblique plate convergence, slip vectors, and forearc deformation. Journal of Geophysical Research 97, 8905–8915.

McClay, K.R., 1989. Analogue Models of Inversion Tectonics. In: Geological Society of London, Special Publications 44, Blackwell Scientific for the Geological Society, Oxford, 41–59.

Mpodozis, C., Ramos, V.A., 1989. The Andes of Chile and Argentina. In: Ericksen, G.E., Cañas, M.T., Reinemud, J.A. (Eds.), Geology of the Andes and its Relation to Hydrocarbon and Mineral Resources. Circum-Pacific Council for Energy and Mineral Resources, Earth Sciences Series 59–90.

Mpodozis, C., Marinovic, N., Smoje, I., Cuitiño, L., 1993. Estudio geológico-estructural de la Cordillera de Domeyko entre Sierra Limón Verde y Sierra Mariposas. Región de Antofagasta. Escala 1:100.000. Informe registrado IR-93-04 Servicio Nacional de Geología y Minería. Corporación Nacional del Cobre de Chile.

Nalpas, T., Györfi, I., Guillocheau, F., Lafont, F., Homewood, P., 1999. Influence de la charge sédimentaire sur le développment d'anticlinaux synsédimentaires. Modélisation analogique et exemple de terrain (bordure sud du bassin de Jaca). Bulletin de la Societe Geologique de France 170, 733–740.

Naranjo, J., Cornejo, P., 1992. Hoja Salar de la Isla. Servicio Nacional de Geología y Mineria, Carta Geológica de Chile, No. 72.

Naylor, M.A., Mandl, G., Sijpesteijn, C.H.K., 1986. Fault geometries in basement-induced wrench faulting under different initial stress states. Journal of Structural Geology 8, 737–752.

Panien, M., Schreurs, G., Pfiffner, A., 2005. Sandbox experiments on basin inversion: testing the influence of basin orientation and basin fill. Journal of Structural of Geology 27, 433–445.

Pardo-Casas, F., Molnar, P., 1987. Relative motion of the Nazca (Farallon) and South American plates since late Cretaceous time. Tectonics 6, 233–248.

Ramberg, H., 1981. Gravity, Deformation, and the Earth's Crust in Theory. Experiments and Geological Applications, second ed. Academic-Press, London, New York.

Ranalli, G., Yin, Z.M., 1990. Critical stress difference and orientation of faults in rocks with strength anisotropies; the two-dimensional case. Journal of Structural Geology 12, 1067–1071.

Ravaglia, A., Turrini, C., Seno, S., 2004. Mechanical stratigraphy as a factor controlling the development of a sandbox transfer zone: a three-dimensional analysis. Journal of Structural Geology 26, 2269–2283.

Reutter, K.J., Chong, G., Scheuber, E., 1993. The "West Fissure" and the Precordilleran Fault System of Northern Chile. Second ISAG. Oxford, UK. 237–240.

Richard, P., 1991a. Experiments on faulting in a two-layer cover sequence overlying a reactivated basement fault with oblique-slip. Journal of Structural Geology 13, 459–469.

Richard, P., Cobbold, P., 1989. Structures en fleur positives et décrochements crustaux: modélisation analogique et interprétation mécanique. Comptes Rendus de l'Académie des Sciences Paris 308 (Série II), 553–560.

Richard, P., 1991b. Experiments on fault reactivation in strike-slip mode. Tectonophysics 188, 117–131.

Sanz de Galdeano, C., Buforn, E., 2005. From strike-slip to reverse reactivation: The Crevillente Fault System and seismicity in the Bullas-Mula area (Betic Cordillera, SE Spain). Geologica Acta 3, 241–250.

Schöpfer, M.P.J., Steyrer, H.P., 2001. Experimental modeling of strike-slip faults and the self-similar behavior. In: Koyi, H.A., Mancktelow, N.S. (Eds.), Tectonic Modeling: A Volume in Honor of Hans Ramberg. Geological Society of America Memoir 193, Geological Society of America, Boulder, Colorado, pp. 21–27.

Schreurs, G., Colletta, B., 1998. Analogue modelling of faulting in zones of continental transpression and transtension. In: Holdsworth, R.E., Strachan, R.A., Dewey, J.F. (Eds.), Continental Transpressional and Transtensional Tectonics. Geological Society of London, Special Publications 135, Geological Society, London, pp. 59–79.

Soto, R., Martinod, J., Riquelme, R., Hérail, G., Audin, L., 2005. Using geomorphological markers to discriminate recent tectonics activity in the Precordillera of North Chilean forearc (24–25°S). Tectonophysics 411, 41–55.

Storti, F., 1997. Simulazione di anticlinalli di rampa e cunei di accrezione mediante modellizzazione analogica. Bolletino della Societá Geologica Italiana 116, 17–38.

Storti, F., McClay, K., 1995. Influence of syntectonic sedimentation on thrust wedges in analogue models. Geology 23, 999–1002.

Tassara, A., 2005. Interaction between the Nazca and South American plates and formation of the Altiplano-Puna plateau: Review of a flexural analysis along the Andean margin (15°–34°S). Tectonophysics 399, 39–57.

Tikoff, B., Teyssier, C., 1994. Strain modelling of displacement-field partitioning in transpressional orogens. Journal of Structural Geology 16, 1575–1588.

Tomlinson, A.J., Mpodozis, C., Cornejo, P.C., Ramirez, C.F., Dimitru, T., 1994. El Sistema de Fallas Sierra Castillo-Agua Amarga: transpresión sinistral eocena en la Precordillera de Potrerillos-El Salvador. Actas VII Congreso Geológico Chileno 2, 1459–1463.

Tondji Biyo, J.J., 1995. Chevauchements et bassins compressifs. Influence de l'érosion et de la sédimentation. Modélisation analogique et exemples naturels. In: Memoir Géosciences Rennes, 59.

Ustaszewski, K., Schumacher, M., Schmid, S.M., Nieuwland, D., 2005. Fault reactivation in brittle–viscous wrench systems-dynamically scaled analogue models and application to the Rhine–Bresse transfer zone. Quaternary Science Reviews 24, 365–382.

Vannucchi, P., 1999. Segmented, curved faults: the example of the Balduini Thrust Zone, Northern Apennines, Italy. Journal of Structural Geology 21, 1655–1668.

Vendeville, B.C., 1987. Champs de failles et tectonique en extension: Modélisation expérimentale. Mémoires et Documents du Centre Armoricain d'Etude Structurale des Socles 15. Ph.D. thesis. University of Rennes I.

Victor, P., Oncken, O., Glodny, J., 2004. Uplift of the western Altiplano plateau: Evidence from the Precordillera between 20° and 21° (northern Chile). Tectonics 23, doi:10.1029/2003TC001519.

Viola, G., Odonne, F., Mancktelow, N.S., 2004. Analogue modelling of reverse fault reactivation in strike–slip and transpressive regimes: application to the Giudicarie fault system, Italian Eastern Alps. Journal of Structural Geology 26, 401–418.

Weijermars, R., Jackson, M.P.A., Vendeville, B., 1993. Rheological and tectonic modeling of salt provinces. Tectonophysics 217, 143–174.

Yin, Z.M., Ranalli, G., 1992. Critical stress difference, fault orientation and slip direction in anisotropic rocks under non-Andersonian stress systems. Journal of Structural Geology 14, 237–244.